Eur Biophys J (2005) 34: 1017–1029
DOI 10.1007/s00249-005-0487-7

ARTICLE

Junying Li · Louisa Stevens · Dennis Wray

Molecular regions underlying the activation of low- and high-voltage activating calcium channels

Received: 30 March 2005 / Accepted: 6 April 2005 / Published online: 28 May 2005

Abstract We have studied two aspects of calcium channel activation. First, we investigated the molecular regions that are important in determining differences in activation between low- and high-voltage activated channels. For this, we made chimeras between the low-voltage activating $Ca_V3.1$ channel and the high-voltage activating $Ca_V1.2$ channel. Chimeras were expressed in oocytes, and calcium channel currents recorded by voltage clamp. For domain I, we found that the molecular region that is important in determining the voltage dependence of activation comprises the pore regions S5-P as well as P-S6, but surprisingly not the voltage sensor S1–S4 region, which might have been expected to play a major part. By contrast, the smaller, but still significant, modulating effects of domain II on activation properties were due to effects involving both S1–S4 and S5–S6 but not the I/II linker. Second, during channel activation we studied movement of the S4 segment in domain I of one of the chimeras, using cysteine-scanning mutagenesis. The reagent parachloromercuribenzensulfonate inhibited currents for mutants V263, A265, L266 and A268, but not for F269 and V271, and voltage dependence of inhibition for residue V263 indicated S4 movement, which occurred before channel opening. The data indicate movement outwards upon depolarisation so as to expose amino acids up to residue 268 in S4.

Keywords Ion channels · Electrophysiology · Ion channel regulation

Junying Li and Louisa Stevens contributed equally to this work.

J. Li · L. Stevens · D. Wray (✉)
School of Biomedical Sciences,
University of Leeds, Leeds,
LS2 9JT, UK
E-mail: d.wray@leeds.ac.uk
Tel.: +44-113-3434320
Fax: +44-113-3434228

Introduction

Voltage-dependent calcium channels have important physiological roles, including cardiac excitation and contraction, neurotransmitter release, and secondary messenger processes. The pore-forming subunit of the calcium channel (α_1) has a structure comprising four homologous domains (I–IV), each with six transmembrane segments (S1–S6) (Catterall 1995; Hofmann et al. 1999; Perez-Reyes 2003; Wray 2000). These channels have been classified by their electrophysiological characteristics, sensitivity to pharmacological agents, and their structure; the Ca_V1 and Ca_V2 families are high-voltage-activating, while the Ca_V3 family is low-voltage-activating.

For potassium and sodium channels, extensive studies of the S4 segment have established that the S4 segment rotates and moves outwards during depolarisation (Bezanilla 2002; Cha and coworkers 1999a, 1999b; Glauner et al. 1999; Larsson et al. 1996; Sheets and Hanck 2002; Yusaf et al. 1996). An alternative model for movement of the S4 by a paddle-like motion has been proposed from structural studies (Jiang et al. 2003). In contrast, very few studies (Garcia et al. 1997; Yamaguchi et al. 1999) have been carried out on the role of the S4 region for calcium channels, and no studies have systematically shown actual movement of the S4 region.

It is not understood at the molecular level why Ca_V3 channels are low-voltage activating, whereas Ca_V1 and Ca_V2 channels are high-voltage activating. In previous work (Li et al. 2004), we started to investigate this issue by constructing a series of chimeras between a low-voltage activating channel $Ca_V3.1$ (α_{1G}) and a high-voltage activating channel $Ca_V1.2$ (α_{1C}). Our data showed that replacing single domains I, III or IV of the $Ca_V3.1$ channel with the corresponding sequence for $Ca_V1.2$ led to a high-voltage activating channel like $Ca_V1.2$. However, replacing domain II of $Ca_V3.1$ with the corresponding domain for $Ca_V1.2$ shifted the current/voltage curve to the high-voltage direction and

modulated the activation kinetics but did not lead to a high-voltage activating channel like $Ca_V1.2$. These results suggest that domains in the calcium channel play different roles in the activation process; domains I, III and IV contribute critically to the difference in voltage dependence of steady-state activation between $Ca_V3.1$ and $Ca_V1.2$. In contrast, domain II, while still contributing appreciably to the voltage dependence of activation, plays more of a modulating role. We also replaced S4 segments in $Ca_V3.1$ by their counterparts in $Ca_V1.2$, but surprisingly the S4 segments were found not to account for the difference in voltage dependence between $Ca_V3.1$ and $Ca_V1.2$ channels. Possible explanations might be that it is the whole of the voltage sensor (i.e. S1–S4) that together determines the voltage sensitivity, or alternatively some other region of the channel, such as the pore, may be involved.

Here we investigated whether it is indeed the whole of the voltage sensor that makes a calcium channel either low-voltage activating or high-voltage activating, or whether another region of the channel is involved. Because domains I and II play different roles in channel opening, we also compared the molecular regions that determine the voltage dependence of activation for these two domains. For this, we created a series of chimeras between $Ca_V3.1$ and $Ca_V1.2$, and we investigated their properties when expressed in oocytes, focusing particularly on steady-state activation. In addition, to show that the S4 segment actually moves upon depolarisation, and to study its extent of movement, we also carried out cysteine-scanning mutagenesis of the S4 segment of domain I, and investigated the accessibility of the cysteine-binding reagent parachloromercuribenzenesulfonate (PCMBS). We employed a high-voltage activating chimeric calcium channel that was not inhibited by PCMBS in the absence of S4 cysteine mutations.

Materials and methods

Materials

The following complemetary DNA (cDNA) clones were used: mouse brain $Ca_V3.1$ (α_{1G}), accession number AJ012569 (Klugbauer et al. 1999); rabbit cardiac $Ca_V1.2$ (α_{1C}), accession number X15539 (Mikami et al. 1989); rat cardiac/brain β_2, accession number M80545 (Perez-Reyes et al. 1992); rabbit skeletal muscle $\alpha_2\delta$, accession number M21948 (Ellis et al. 1988). Restriction enzymes were obtained from Promega, WI, USA and New England Biolabs, Beverly, MA, USA, and chemical reagents were from Sigma, MO, USA.

Construction of chimeras and mutants

All chimeras were made by replacing regions in domains I or II of $Ca_V3.1$ by the corresponding regions in $Ca_V1.2$, as shown in Fig. 1. The chimeras were constructed using standard PCR overlap extension as described before (Horton et al. 1989; Li et al. 2004). For chimera I-S(1–4)C, residues 81–199 of $Ca_V3.1$ were replaced by residues 154–286 of $Ca_V1.2$; for chimera I-S(5–6)C, residues 200–398 of $Ca_V3.1$ were replaced by

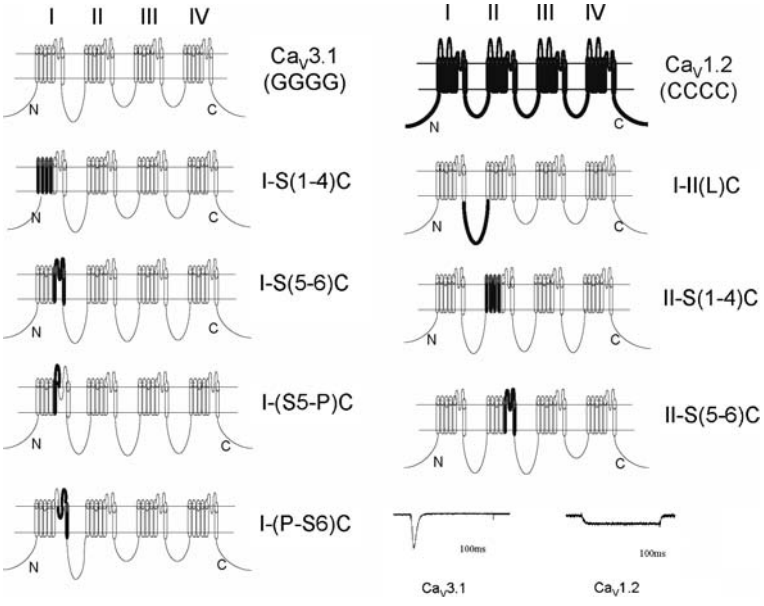

Fig. 1 Schematic structure of wild-type and chimeric channels. Structures are shown for wild-type $Ca_V3.1$ (*thin lines*, GGGG) and $Ca_V1.2$ (*thick lines*, CCCC) channels. Chimeras were made by swapping regions of $Ca_V3.1$ with the corresponding regions of $Ca_V1.2$, as follows. For domain I: chimera I-S(1–4)C by swapping S1–S4, chimera I-S(5–6)C by swapping S5–S6, chimera I-(S5-P)C by swapping S5-P, and chimera I-(P-S6) by swapping P-S6. For the linker: chimera I–II(L)C by swapping the I/II linker. For domain II: chimera II-S(1–4)C by swapping S1–S4, chimera II-S(5–6) by swapping S5–S6. Current traces are also shown for wild-type $Ca_V3.1$ (at −30 mV, *left*) and $Ca_V1.2$ (at +10 mV, *right*); these are the mean of the normalised (at the maximum) currents for 36 and 40 cells, respectively

residues 287–438 of $Ca_V1.2$; for chimera I-(S5-P)C, residues 200–335 of $Ca_V3.1$ were replaced by residues 287–374 of $Ca_V1.2$; for chimera I-(P-S6)C, residues 336–398 of $Ca_V3.1$ were replaced by residues 375–438 of $Ca_V1.2$. In the final PCR products, all chimeric fragments of the four constructs just described contained *Ksp*I and *Hin*dIII restriction sites in the $Ca_V3.1$ sequence on either side of the $Ca_V1.2$ sequence. These chimeric PCR fragments were digested with these enzymes, yielding a 1,103-bp product for I-S(1–4)C, a 920-bp product for I-S(5–6)C, a 917-bp product for I-(S5-P)C, and a 1,064-bp product for I-(P-S6)C. The digested fragments were ligated with the similarly digested wild-type $Ca_V3.1$ (in PGEM-HEL vector, Li et al. 2004).

For chimera II-S(1–4)C, residues 742–856 of $Ca_V3.1$ were replaced by residues 553–672 of $Ca_V1.2$; for chimera II-S(5–6)C, residues 857–967 of $Ca_V3.1$ were replaced by residues 673–786 of $Ca_V1.2$. The final PCR fragments of these two chimeras included *Spe*I and *Sfi*I restriction sites in the $Ca_V3.1$ sequence on either side of the $Ca_V1.2$ sequence. After digestion with these enzymes, a 1,264-bp product for II-S(1–4)C and a 1,258-bp product for II-S(5–6)C were inserted into wild-type $Ca_V3.1$(in PGEM-HEL vector) after digestion with the same enzymes.

For chimera I–II(L)C, residues 399–741 of $Ca_V3.1$ were replaced by residues 439–552 of $Ca_V1.2$; the chimeric PCR fragments had *Csp*45I and *Bsa*AI restriction sites. After digestion of the 1,461-bp products with these enzymes, the fragment was ligated into a similarly digested construct: "$Ca_V3.1$(*Xba*I-*Eco*RI)-pUC18". The latter construct is a subclone of wild-type $Ca_V3.1$, and was previously made (Li et al. 2004) by inserting the *Xba*I-*Eco*RI subfragments of $Ca_V3.1$ (4,391 bp) into the pUC18 vector. Then the whole insert for the I/II(L)C chimera was transferred to $Ca_V3.1$-PGEM-HEL after *Xba*I and *Eco*RI digestion.

All cysteine mutants were constructed in the S4 region of domain I of the chimera CGGG in pGEM-HEL (Li et al. 2004). For this, a 1,380-bp fragment of chimera CGGG was first subcloned into pUC18 vector using restriction enzymes *Xba*I and *Hin*dIII. Site-directed mutagenesis was then performed on this smaller construct using the QuickChange (Stratagene) method, and the mutated insert was subcloned back into wild-type $Ca_V3.1$ in PGEM-HEL to reconstruct the CGGG chimera. The entire inserts were verified by DNA sequencing.

All joins and the entire PCR inserts of all constructs were verified by DNA sequencing. For making RNA, $Ca_V3.1$ and chimeric cDNAs (in pGEM-HEL) were linearised with *Mlu*I; $Ca_V1.2$ (in pcDNA3) was linearised with *Asp*718; β_2 and $\alpha_2\delta$ (both in pcDNA3) were linearised with *Not*I; capped cRNAs were synthesised in vitro using T7 MEGAscript (Ambion).

Electrophysiological recording

Xenopus oocytes were injected with a volume of 50 nl containing 10–20 ng wild-type or chimeric α_1 subunit cRNA together with 5 ng β_2 cRNA and 5 ng $\alpha_2\delta$ cRNA. Auxiliary subunits were co-injected because they increase current amplitudes, even for $Ca_V3.1$ (Perez-Reyes 2003). Oocytes were incubated at 19.6°C for 2–4 days in modified Barth's solution (Li et al. 2004). For electrophysiological recordings, cells were perfused with high barium solution [40 mM $Ba(OH)_2$, 50 mM NaOH, 2 mM KOH and 5 mM *N*-(2-hydroxyethyl)piperazine-*N*′-ethanesulfonic acid, adjusted to pH 7.4 by methanesulfonic acid]. Calcium channel currents were recorded at 22–25°C using two-electrode voltage clamp as described previously (Li et al. 2004). Currents were filtered at 2 kHz and sampled at 4 kHz. The membrane potential of the oocytes was held at −80 mV (unless stated otherwise) and 500-ms test depolarisations were applied in 10-mV increments at 0.1 Hz. Peak amplitudes were measured, and current–voltage (I/V) relationships were constructed, with leak subtraction as previously described (Li et al. 2004). The I/V curves were fitted with the Boltzmann equation $I = (V - V_{rev})G_{max}/[1+\exp(V_{0.5} - V)/k]$, where I is the peak current, V the test potential, V_{rev} the reversal potential, G_{max} the maximum conductance, $V_{0.5}$ the half-maximal activation potential, and k is the slope parameter. The PCMBS (a membrane-impermeable cysteine binding reagent) was applied by continuous perfusion during repetitive stimulation at 0.1 Hz (pulse duration 200 ms) from a holding potential of −80 mV with pulses to either −30 mV for $Ca_V3.1$ or +10 mV for CGGG. To investigate the effect of holding potential on PCMBS action, the following protocol was used. An I/V curve was first obtained as previously described at a holding potential of −80 mV, then the cell was held at the required holding potential without any depolarising pulses while PCMBS (100 μM) was applied for 6 min, followed by washing for 2 min; finally the holding potential was returned to −80 mV and a further I/V curve obtained. Data are given as the mean ± the standard error, and statistical significance was calculated using Student's paired t test or analysis of variance as appropriate, with $p < 0.05$ as the significant level.

To test for "endogenous" currents in the presence of auxiliary subunits (i.e. due to auxiliary subunits combining with endogenous α_1), the β and $\alpha_2\delta$ subunits were injected alone (i.e. without the α_1 subunit); the endogenous currents were not large (-0.07 ± 0.02 μA, $n = 3$). Furthermore, in experiments with $Ca_V1.2$ injected with β and $\alpha_2\delta$, the residual current after blocking by nifedipine (1 μM) was -0.05 ± 0.01 μA ($n = 3$), which is also a separate estimate of the endogenous current, as the latter is insensitive to dihydropyridines (Singer et al. 1991). Thus, in our hands, the size of the endogenous current (i.e. in the presence of just auxiliary subunits) is similar to some estimates (De Waard and Campbell 1995; Singer et al. 1991), although smaller than other estimates (Lacerda et al. 1994; Scholze et al. 2001). The small size of our endogenous currents may be because our experiments were carried out after injection for only 2–4 days, or because the rabbit $\alpha_2\delta$ (used here) may boost currents less than the rat form, or because high expression vectors

were not used for the auxiliary subunits. The endogenous current was generally much less than 25–30% of currents with injected α_1 subunits (see figure legends). The lack of marked endogenous currents is also apparent because when currents were small, the kinetics was not uniform; either transient or sustained currents were obtained depending on the channel being expressed (e.g. Fig. 2a compared with b). Finally, contamination from calcium-activated chloride channels was minimised by using chloride-free solutions and by recording barium currents (up to 2 μA); there was no evidence of unexpected tail currents.

Results

Roles of molecular regions in domain I on voltage-dependence of activation

We have previously shown that replacement of domain I in $Ca_V3.1$ by $Ca_V1.2$ transforms the channel from low-voltage activating (like $Ca_V3.1$) to high-voltage activating (like $Ca_V1.2$) (see "Introduction"). In order to investigate which molecular region of domain I contributes to determining the voltage dependence of

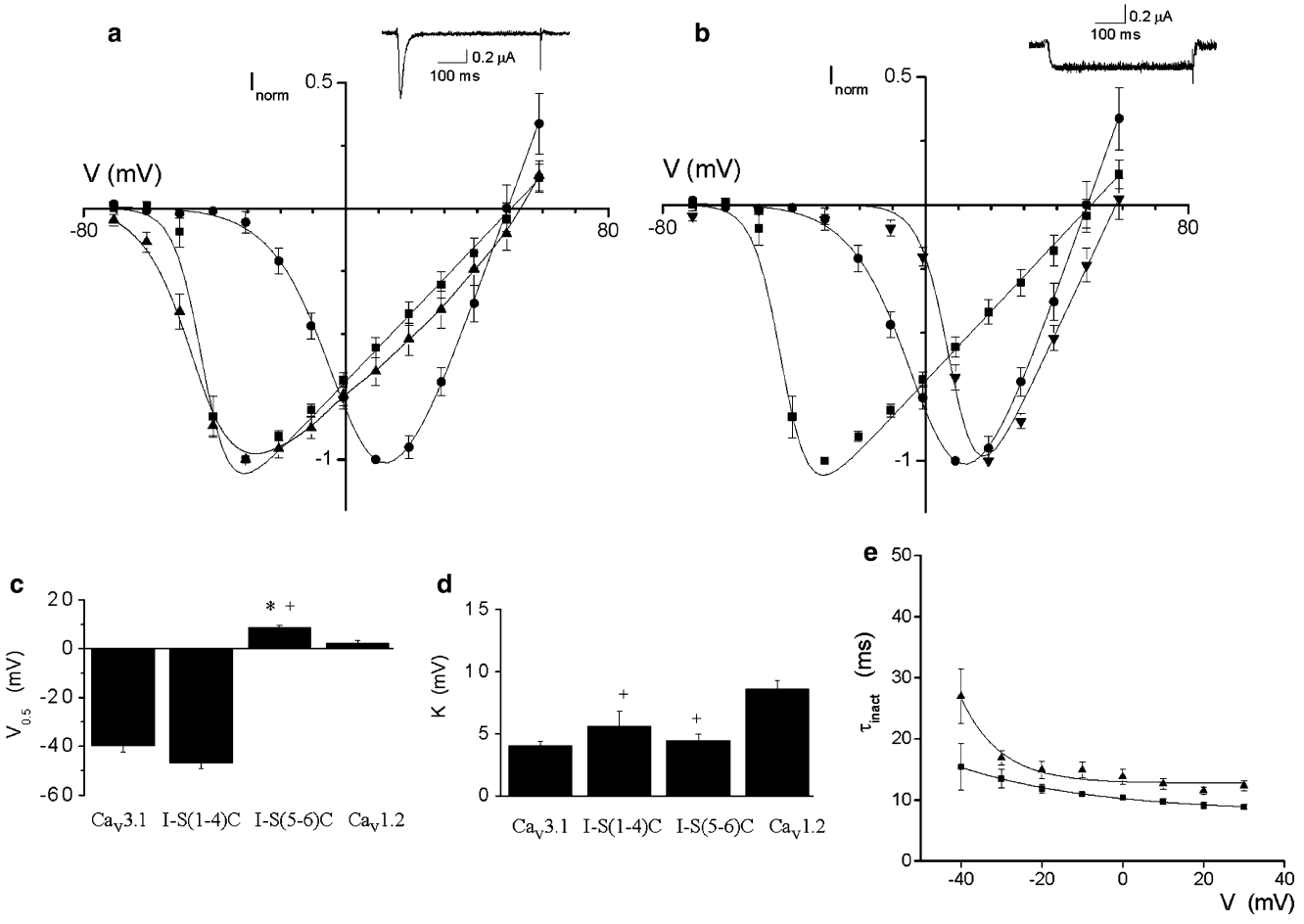

Fig. 2 The roles of S1–S4 and S5–S6 regions of domain I in determining differences in voltage dependence of activation between $Ca_V3.1$ and $Ca_V1.2$. **a** The mean value of peak-normalised currents (I_{norm}) for chimera I-S(1–4)C (*triangles*, $n=7$), wild-type $Ca_V3.1$ (*squares*, $n=7$) and $Ca_V1.2$ (*circles*, $n=8$) against the test potential, V, with normalisation to the current at −30 mV (−0.35 ± 0.09 μA) for I-S(1–4)C, at −30 mV (−0.85 ± 0.21 μA) for $Ca_V3.1$, and at +10 mV (−0.26 ± 0.08 μA) for $Ca_V1.2$. The mean values of the normalised currents were fitted with the Boltzmann curves shown. A sample current trace for the I-S(1–4)C chimera with a voltage step to −30 mV is shown in the *inset*. **b** The mean value of normalised currents for chimera I-S(5–6)C (*triangles*, $n=9$) against the test potential, V, with normalisation to the value at +20 mV (−0.23 ± 0.02 μA), and fitted with the Boltzmann curves shown. For comparison, the data for wild-type channels are also shown in this and the subsequent figures, using the same curves and the same symbols as in **a**. A sample current trace for I-S(5–6)C is shown in the *inset* (voltage step to +20 mV). **c**, **d** The Boltzmann parameters $V_{0.5}$ and k are shown for chimeras I-S(1–4)C and I-S(5–6)C and wild-type controls. For this, the Boltzmann parameters were first fitted to the I/V curve for each individual cell, then the mean values were obtained by averaging $V_{0.5}$ and k over the number of cells. An *asterisk* indicates significant difference ($p<0.05$) compared with wild-type $Ca_V3.1$; a *plus sign* indicates significant difference from wild-type $Ca_V1.2$. **e** The mean values of the inactivation time, τ_{inact}, against the test potential, V, for wild-type $Ca_V3.1$ (*squares*, $n=7$), and chimera I-S(1–4)C (*triangles*, $n=7$), again fitted with the single-exponential curves shown. The data are shown as mean ± the standard error of the mean in this and in subsequent figures. Boltzmann and exponential fitting and analysis were carried out similarly for the data shown in subsequent figures

activation, we constructed chimeras in domain I, replacing regions in $Ca_V3.1$ with corresponding regions from $Ca_V1.2$. Channels were expressed in oocytes, and recordings made by two-electrode voltage clamp.

For chimera I-S(1–4)C, which has the S1–S4 region of domain I $Ca_V3.1$ replaced by that of $Ca_V1.2$ (Fig. 1), the calcium channel currents were low-voltage activating, with an I/V curve similar to that for $Ca_V3.1$ (Fig. 2a). Indeed, the Boltzmann parameters $V_{0.5}$ and k were not significantly different from the values for $Ca_V3.1$, but were significantly different from the values for $Ca_V1.2$ (Fig. 2c, d). Channel currents for the chimera were fast-inactivating like $Ca_V3.1$ although somewhat slower (Fig. 2e), but still markedly different from the non-inactivating $Ca_V1.2$ currents (Figs. 1, 2, sample traces). Thus, the S1–S4 region of domain I does not contribute to determining differences in activation between these low-voltage and high-voltage activating channels, and has only a weak modulating effect on inactivation.

In contrast, for chimera I-S(5–6)C, with the S5–S6 region of domain I of $Ca_V3.1$ replaced by $Ca_V1.2$ (Fig. 1), the currents were high-voltage activating, with an I/V curve qualitatively similar, although not identical, to that for $Ca_V1.2$ (Fig. 2b) ($V_{0.5}$ was even higher than for $Ca_V1.2$, although k was similar to $Ca_V3.1$, Fig. 2c, d). Also, the currents were non-inactivating (Fig. 2, sample trace), as for $Ca_V1.2$. Hence, it is the S5–S6 region of domain I (rather than S1–S4) that contributes strongly to determining not only the differences in the voltage dependence of activation between the low-voltage and high-voltage activating channels, but also determines inactivation properties.

To narrow down the molecular region in S5–S6 of domain I that is important for these properties, we constructed two further chimeras with the $Ca_V1.2$ sequence replacing that of $Ca_V3.1$ as follows: from S5 to the beginning of the P helix [chimera I-(S5-P)C], and from the P helix (via the selectivity filter) to the end of S6 [chimera I-(P-S6)C] (Fig. 1). The calcium channel currents for both these chimeras were high-voltage-activating, with I/V curves closest to, but not identical to, that for $Ca_V1.2$ (Fig. 3a, b) (again, the values for $V_{0.5}$ were even higher than for $Ca_V1.2$, Fig. 3c, while k values were either like those of $Ca_V1.2$ [I-(S5-P)C] or $Ca_V3.1$ [I-(P-S6)C], Fig. 3d). Taken together, these results are surprising because one might have expected only one of these regions to be responsible for determining voltage-activation properties. Therefore, it seems that both regions (i.e. S5-P and P-S6) must act synergistically to give a low-voltage activated channel; replacing just one of these regions gives a high-voltage activated channel.

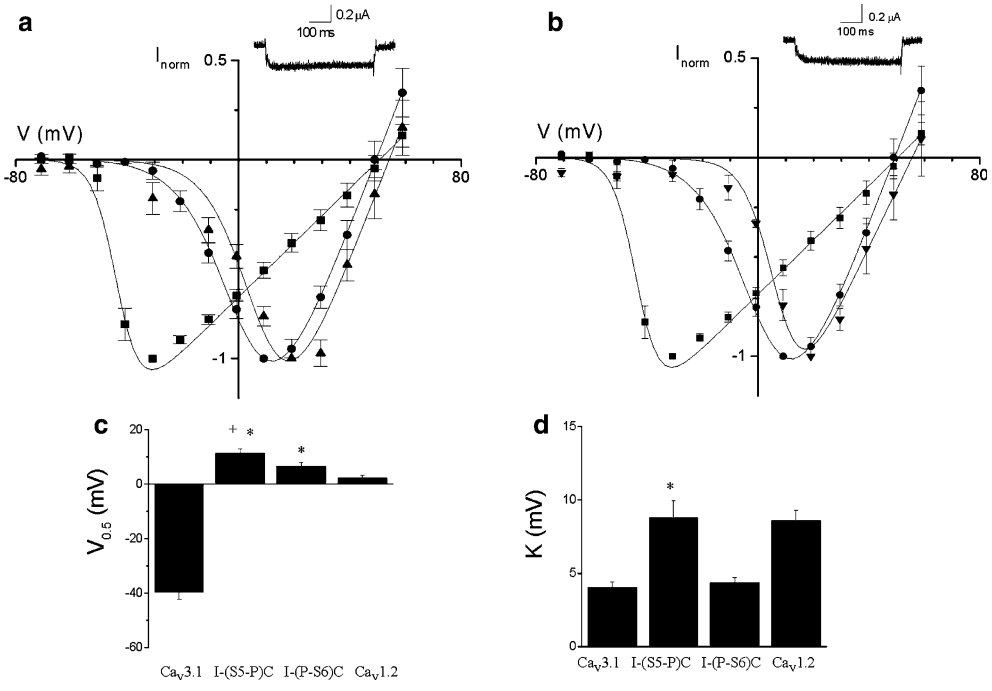

Fig. 3 The roles of S5-P and P-S6 regions in determining differences in the voltage dependence of activation between $Ca_V3.1$ and $Ca_V1.2$. **a** The normalised I/V curve is shown for chimera I-(S5-P)C (*triangles*, $n=6$), with normalisation to the current at +20 mV (-0.23 ± 0.03 µA). For comparison, the data for wild-type $Ca_V3.1$ (*squares*) and $Ca_V1.2$ (*circles*) are also shown (data as in Fig. 2a). A sample current trace for I-(S5-P)C with a voltage step to +20 mV is shown (*inset*). **b** The normalised I/V curve is shown for chimera I-(P-S6)C (*triangles*, $n=5$), with normalisation to the current value at +20 mV (-0.20 ± 0.03 µA). Data for wild-type $Ca_V3.1$ (*squares*) and $Ca_V1.2$ (*circles*) are again shown as before. A sample current trace for I-(P-S6)C (voltage step to +20 mV) is also shown (*inset*). **c**, **d** The Boltzmann parameters $V_{0.5}$ and k are shown for chimeras I-(S5-P)C and I-(P-S6)C as well as for wild type controls. An *asterisk* indicates significant difference ($p<0.05$) compared with wild-type $Ca_V3.1$; a *plus sign* indicates significant difference from wild-type $Ca_V1.2$

Similarly, currents were non-inactivating for both chimeras (sample traces, Fig. 3), again indicating the roles of both regions. Thus, we conclude that, for domain I, both the S5-P region (i.e. S5 plus a linker to the start of the P helix region) and the P-S6 region (i.e. P helix–selectivity filter–S6 region) contribute to determining the voltage dependence of activation, as well as determining inactivation.

Roles of molecular regions in domain II on voltage dependence of activation

We have previously shown that domain II, in contrast to domain I, only contributes to a smaller, but significant, extent to the differences in the voltage dependence of activation between $Ca_V1.2$ and $Ca_V3.1$ channels (see "Introduction"): replacement of domain II (including the I–II linker) of $Ca_V3.1$ with the corresponding sequence for $Ca_V2.1$ (chimera "GCGG", Li et al. 2004) shifts the I/V curve to the right by up to 15 mV, but not so far to the right as to be high-voltage activating like wild-type $Ca_V1.2$ with its shift greater than 40 mV. Here we have investigated which molecular region underlies these effects, starting with a study of the I/II linker.

For this, we swapped the I–II linker of $Ca_V3.1$ with the corresponding regions of $Ca_V1.2$, forming chimera I–II(L)C (Fig. 1). Surprisingly, this chimera activated at more hyperpolarised potentials than for $Ca_V3.1$, with the I/V curve shifted to the left (Fig. 4a) and the $V_{0.5}$ value significantly more negative than for $Ca_V3.1$, although the k value remained similar to that for $Ca_V3.1$ (Fig. 4b, c). Thus, the data for this chimera show that the I–II linker did not account for the activation properties seen with chimera GCGG, and so the I/II linker does not have a fundamental role in determining whether the channel is low-voltage activating or high-voltage activating. Since chimera I–II(L)C introduced a β-binding site from $Ca_V1.2$, the leftward shift could in principle be due to the shift that the β subunit causes in $Ca_V1.2$ (although not for $Ca_V3.1$) (reviewed in Perez-Reyes 2003; Walker and De Waard 1998). However, when we expressed this chimera in the absence of $\alpha_2\delta/\beta_2$ subunits, the voltage for half-maximal activation ($V_{0.5} = -58.1 \pm 3.6$ mV; $n = 7$) was not significantly different from its value in the presence of subunits, indi-

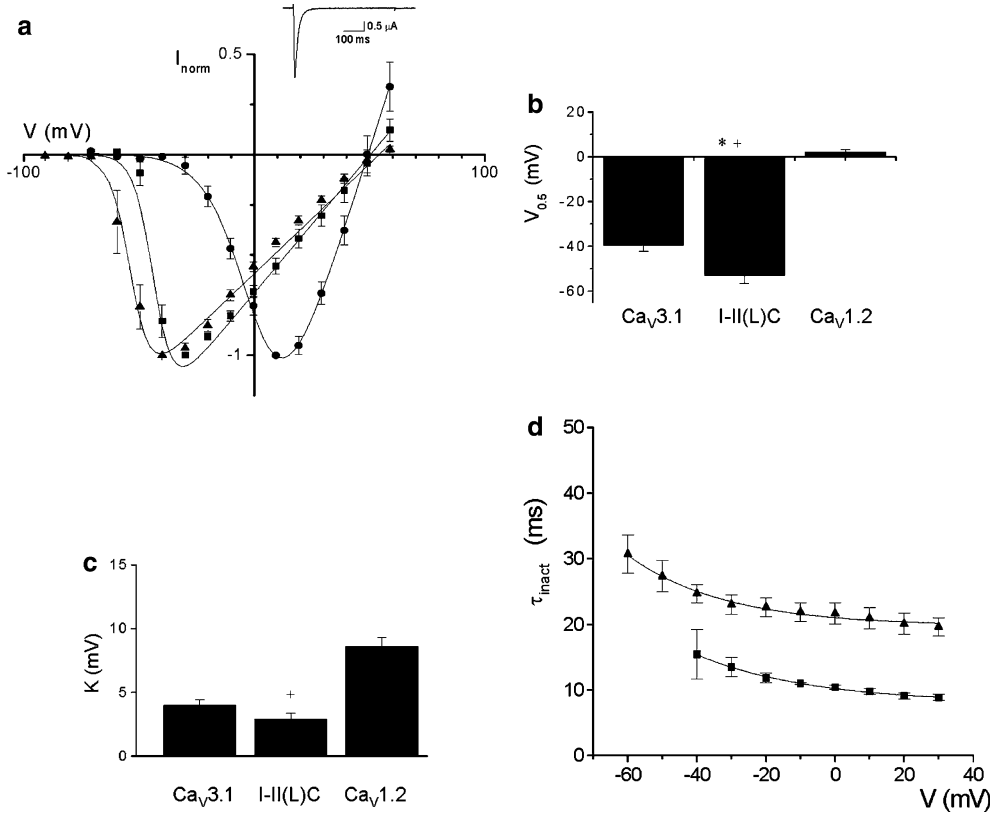

Fig. 4 The role of the I/II linker in determining differences in the voltage dependence of activation between $Ca_V3.1$ and $Ca_V1.2$. **a** The normalised I/V curve is shown for chimera I–II(L)C (*triangles*, $n = 7$), with normalisation to the current at −40 mV (-2.24 ± 0.68 µA). For comparison, the curves for wild-type $Ca_V3.1$ (*squares*) and $Ca_V1.2$ (*circles*) are again shown using the same data as in Fig. 2a. A sample current trace for I–II(L)C with subunits is shown (*inset*) for a voltage step to −40 mV. **b**, **c** The Boltzmann parameters $V_{0.5}$ and k are shown for chimera I–II(L)C in comparison with wild-type controls. An *asterisk* indicates significant difference ($p < 0.05$) compared with wild-type $Ca_V3.1$; a *plus sign* indicates significant difference from wild-type $Ca_V1.2$. **d** The inactivation time constant, τ_{inact}, against the test potential for chimera I–II(L)C (*triangles*, $n = 7$), together with $Ca_V3.1$ (*squares*) (same data as in Fig. 2e)

cating that the observed shift (with respect to $Ca_V3.1$) for chimera I–II(L)C was not due to an effect of the β subunit. Inactivation of the chimera was transient, like $Ca_V3.1$ (sample trace, Fig. 4), although the inactivation time constant was about twofold larger than for $Ca_V3.1$ (Fig. 4d), suggesting a modulating role only for the I/II linker in inactivation.

To investigate the possible role in activation of other regions of domain II, chimeras II-S(1–4)C and II-S(5–6)C were made by replacing the S1–S4 region or the S5–S6 region, respectively, in domain II of $Ca_V3.1$ with the corresponding region of $Ca_V1.2$ (Fig. 1). It can be seen (Fig. 5a, b) that the I/V curves of both these chimeras were shifted to the right as compared with that for $Ca_V3.1$, but again not so far to the right as to be similar to $Ca_V1.2$; indeed the $V_{0.5}$ values (Fig. 5c) were intermediate in value between those of the two wild-type channels (although the k values were closer to the values for $Ca_V1.2$, Fig. 5d). Therefore, taken together, both the S1–S4 region and the S5–S6 region contribute to the effects of domain II on activation processes in these channels. The currents for both the chimeras were transient and inactivating in nature (sample traces, Fig. 5), basically like $Ca_V3.1$, although somewhat slower (Fig. 5e), indicating that the effect of domain II on inactivation is less marked than for S5–S6 of domain I.

Effects of PCMBS on domain I S4 cysteine mutants

We first tested whether PCMBS reacts with the low-voltage activating wild-type $Ca_V3.1$ channels. Oocytes expressing these channels were repetitively depolarised (see "Materials and methods") from a holding potential of −80 mV, and PCMBS (100 μM) was applied during continuous perfusion. As can be seen (Fig. 7a), PCMBS inhibited currents for wild-type $Ca_V3.1$, indicating that native cysteines have reacted; indeed there are 14 cysteines present in extracellular loops of wild-type $Ca_V3.1$. Because of this reactivity with PCMBS, $Ca_V3.1$ could not be used for cysteine-scanning mutagenesis. However, many of the extracellular cysteines for $Ca_V3.1$ are located on extracellular loops of domain I (seven cysteines), whereas $Ca_V1.2$ possesses only four cysteines in this domain. Therefore, we tested chimera CGGG, with domain I of $Ca_V3.1$ replaced by $Ca_V1.2$. For this

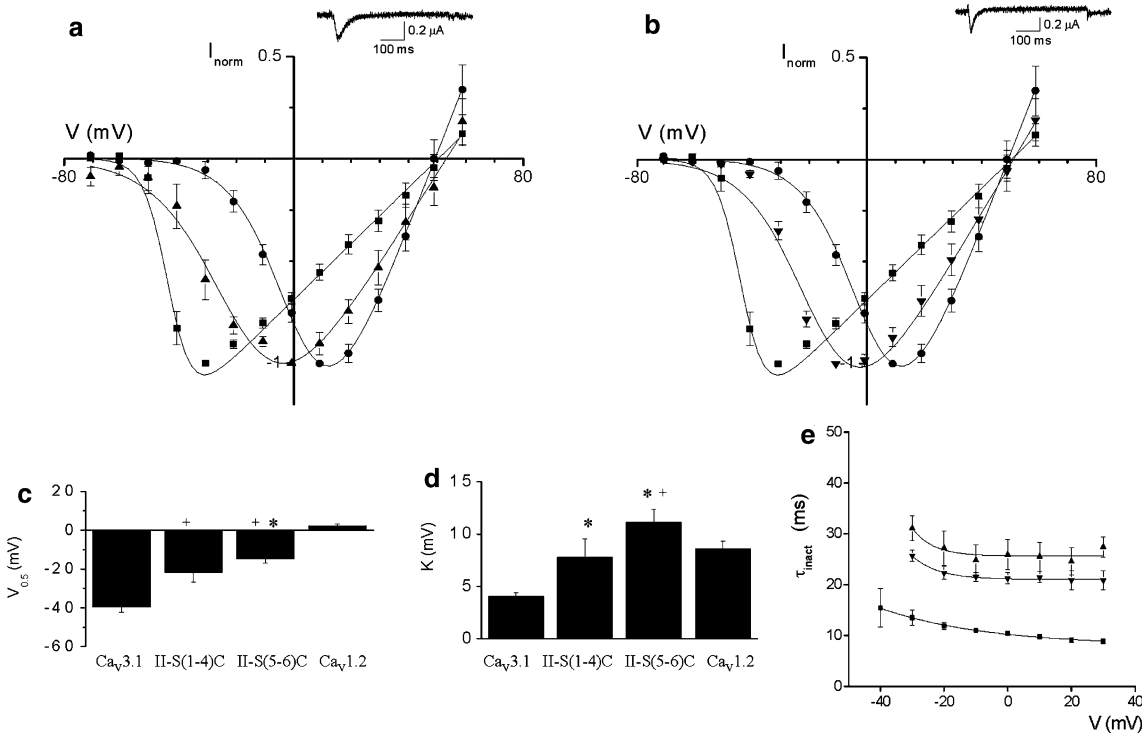

Fig. 5 The role of S1–S4 and S5–S6 regions of domain II in determining differences in the voltage dependence of activation between $Ca_V3.1$ and $Ca_V1.2$. **a** The normalised I/V curve is shown for chimera II-S(1–4)C (*triangles* $n=5$), with normalisation to the value at 0 mV (-0.23 ± 0.03 μA). The same data as in Fig. 2a are also shown for wild-type $Ca_V3.1$ (*squares*) and $Ca_V1.2$ (*circles*) channels. A sample current trace for II-S(1–4)C is shown (*inset*), with a voltage step to 0 mV. **b** The normalised I/V curve is shown for chimera II-S(5–6)C (*triangles*, $n=7$), with normalisation to the current value at −10 mV (-0.41 ± 0.10 μA). For comparison, the curves for wild-type $Ca_V3.1$ (*squares*) and $Ca_V1.2$ (*circles*) are again shown. A sample current trace for chimera II-S(5–6)C (voltage step to −10 mV) is shown (*inset*). **c**, **d** The Boltzmann parameters $V_{0.5}$ and k are shown for chimeras II-S(1–4)C and II-S(5–6)C, as well as wild-type controls. An *asterisk* indicates significant difference ($p<0.05$) from wild-type $Ca_V3.1$; a *plus sign* indicates significant difference from wild-type $Ca_V1.2$. **e** The inactivation time constant, τ_{inact}, against the test potential, for chimeras II-S(1–4)C (*up triangles*, $n=5$) and II-S(5–6)C (*inverted triangles*, $n=7$). For comparison, wild-type $Ca_V3.1$ (*squares*) is also shown (same data as in Fig. 2e)

chimera, PCMBS indeed did not affect currents (Fig. 7b). Therefore, chimera CGGG was suitable for carrying out cysteine-scanning mutagenesis. As previously shown (Li et al. 2004), this chimera is high-voltage activating, and non-inactivating (Fig. 7b).

In order to characterise the movement of the S4 segment in domain I of chimera CGGG, we replaced neutral residues (one at a time) with cysteines (Fig. 6b). After the mutants had been expressed in oocytes, PCMBS (100 μM) was applied during repetitive stimulation from a holding potential of −80 mV. The results show that currents for mutants F269C and V271C were not inhibited by PCMBS (Fig. 8e, f), but currents for mutants V263C, A265C, L266C and A268C were inhibited by the reagent (Fig. 8a–d; $Ca_V1.2$ residue numbering used throughout). Thus, taken together, the data indicate that, under these depolarising conditions, exposure of the S4 region occurs up to and including residue 268, with residues 269 and 271 remaining buried in the membrane.

The *I*/*V* curves before the application of PCMBS were similar for all cysteine mutants when compared with the non-mutated CGGG chimera (data not shown). For those mutants that were inhibited by PCMBS, the rate of inhibition did not vary systematically with the depth of the residue in the membrane (Fig. 8g). This contrasts with the Shaker channel where deeper residues reacted more slowly with PCMBS (Yusaf et al. 1996).

We further examined the effect of PCMBS on the V263C mutant as a function of membrane potential. For this, oocytes expressing the V263C mutated channel were held at various holding potentials in the absence of depolarising pulses (see "Materials and methods") and were treated with PCMBS (100 μM). At a holding potential of −140 mV (Fig. 9a), there was no inhibition of calcium channel currents by PCMBS, indicating that this residue is buried in the membrane at this hyperpolarised potential. For more depolarised holding potentials, an increase in the extent of inhibition by PCMBS was seen (Fig. 9b–e). Therefore, these data show that residue 263 is accessible at depolarised, but not hyperpolarised potentials, implying that depolarisation causes this residue in S4 to move from a position within the membrane to an extracellular location.

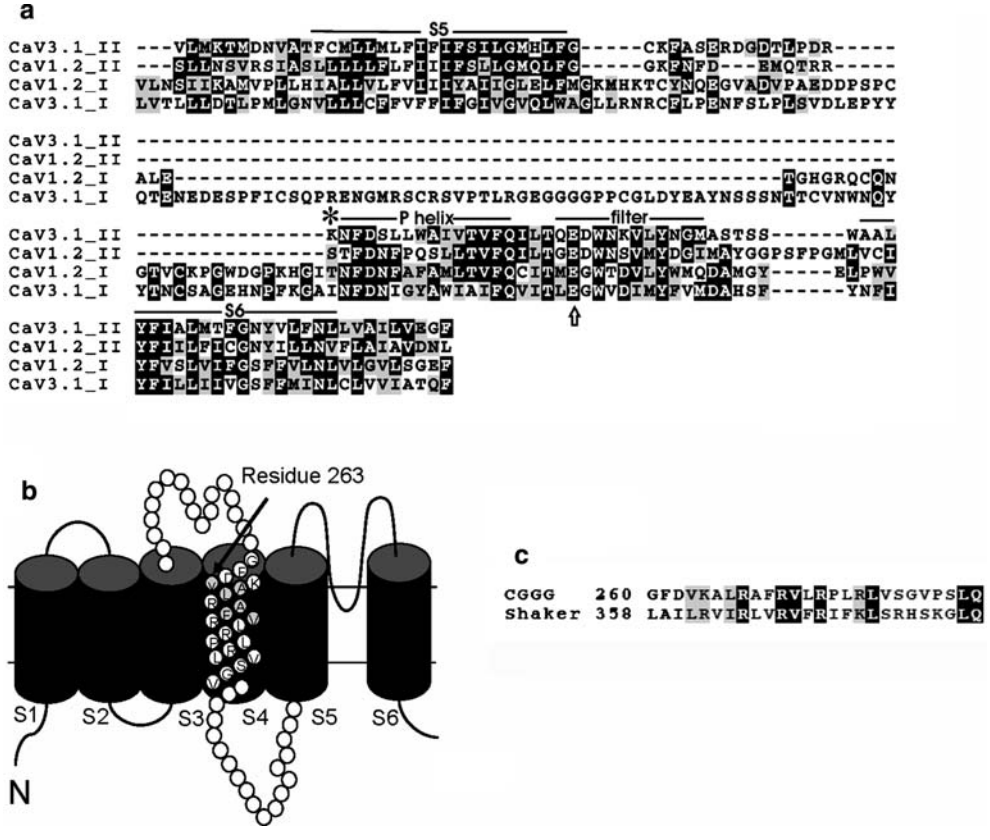

Fig. 6 Amino acid sequences and alignments. **a** Alignment of domains I and II of $Ca_V1.2$ and $Ca_V3.1$. The sequences shown are for the swapped regions of the S5–S6 chimeras. The region swapped for chimera I-(P-S6)C is from the beginning of the P helix (marked with an *asterisk*) to the end of the sequence; the region swapped for I-(S5-P)C covered the remaining sequence shown. The approximate positions of the predicted P helix and selectivity filter are shown as guidelines only. These were obtained by homology modelling against KvAP (1ORS, Jiang et al. 2003) using Jigsaw at http://www.bmm.icnet.uk/~3djigsaw/, and the approximate position of the P helix was also obtained from secondary structure predictions using Jpred at http://www.compbio.dundee.ac.uk/~www-jpred/. The pore glutamate (Talavera and coworkers 2001, 2003) is indicated with an *arrow*. **b** Membrane topology of domain I for chimera CGGG showing positions of the cysteine substitutions (*shaded*) in S4. **c** Sequence alignment of S4 of domain I of the CGGG chimera with the Shaker S4 domain. The residue numbering for domain I of CGGG is as in wild-type $Ca_V1.2$

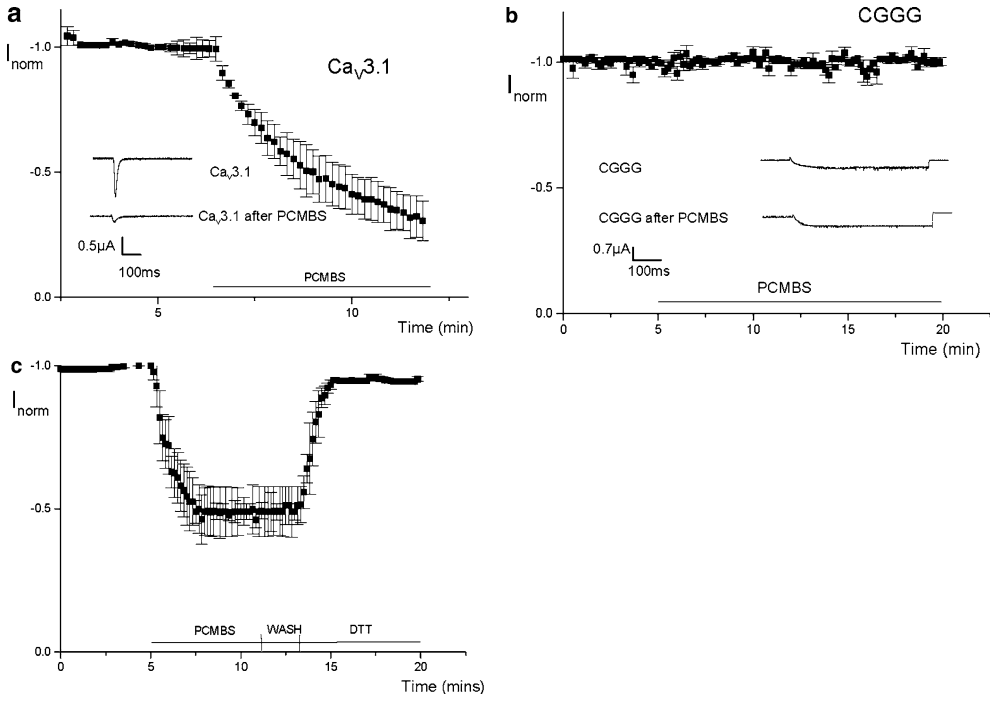

Fig. 7 Effects of parachloromercuribenzenesulfonate (*PCMBS*) on calcium channels without cysteine mutations. **a** The effect of application of PCMBS (100 μM, indicated by the *bar*) on wild-type $Ca_V3.1$ (*squares*, $n=4$) during repetitive depolarisations from −80-mV holding potential (see "Materials and methods"). Current amplitudes were normalised (I_{norm}) with respect to the initial value (-1.15 ± 0.04 μA). Sample current traces are shown at −30-mV depolarisation. **b** The effect of application of PCMBS (100 μM, indicated by the *bar*) on chimera CGGG (*squares*, $n=4$) during repetitive depolarisations from −80-mV holding potential. Current amplitudes were normalised (I_{norm}) with respect to the initial value (-0.76 ± 0.01 μA). Sample current traces are shown at +10-mV depolarisation. **c** Reversal of inhibition of V263C by PCMBS with dithiothreitol (*DTT*). Mean currents are shown for cells expressing the mutant V263C ($n=4$) with repetitive depolarisations from a holding potential of −80 mV (see "Materials and methods"). The PCMBS (100 μM) was applied, followed by washing and then DTT (1 mM), as shown by the *solid lines*. The current (I_{norm}) was normalised to the initial value (-1.16 ± 0.07 μA)

Finally, to establish that the inhibitory effect of PCMBS was due to specific binding to a cysteine residue, we tested this by applying PCMBS followed by 1 mM dithiothreitol. As can be seen in Fig. 7c, dithiothreitol (but not washing) indeed reversed the inhibition of PCMBS on mutant V263C, consistent with specific covalent binding of PCMBS to the cysteine.

Discussion

For domain I, with its large influence on activation properties, we found that the voltage sensor S1–S4 region does not contribute to determining differences in activation properties between high-voltage activated and low-voltage activated channels; rather we showed that it is the pore S5–S6 region that is involved. Furthermore, we showed that residues within both sections of the domain I pore region (i.e. the region of S5 plus its linker to the start of the P helix, and the region of P helix–selectivity filter–S6) are involved, *both* these regions acting synergistically to give a low-voltage activating channel. We also showed that the intracellular I/II linker does not determine whether the channel is high-voltage activating or low-voltage activating, and in fact this chimera gave an unexpected hyperpolarising shift. For domain II, with its somewhat smaller influence on determining activation properties, both the S1–S4 and the S5–S6 regions contributed.

Our conclusion that the voltage sensor S1–S4 region of domain I does not contribute to determining these differences in activation properties is consistent with our earlier work showing that the S4 region itself of domain I does not determine the voltage dependence of activation (Li et al. 2004). Furthermore, it is also consistent with data on gating currents for calcium channels, where gating currents precede activation of high-voltage activated channels by 30–40 mV, but by 10 mV for low-voltage activated channels, indicating that the voltage sensor moves at rather similar voltages independent of whether the channel is low-voltage activating or high-voltage activating (Josephson 1997; Lacinova et al. 2002; Neely et al. 1993).

On the other hand, since our data indicate that residues within the pore region of domain I determine the voltage dependence of activation, this suggests that the key step for determining differences in the voltage dependence of activation in these calcium channels is concerned with either (1) the voltage dependence of the coupling between voltage sensor and gate, or (2) the

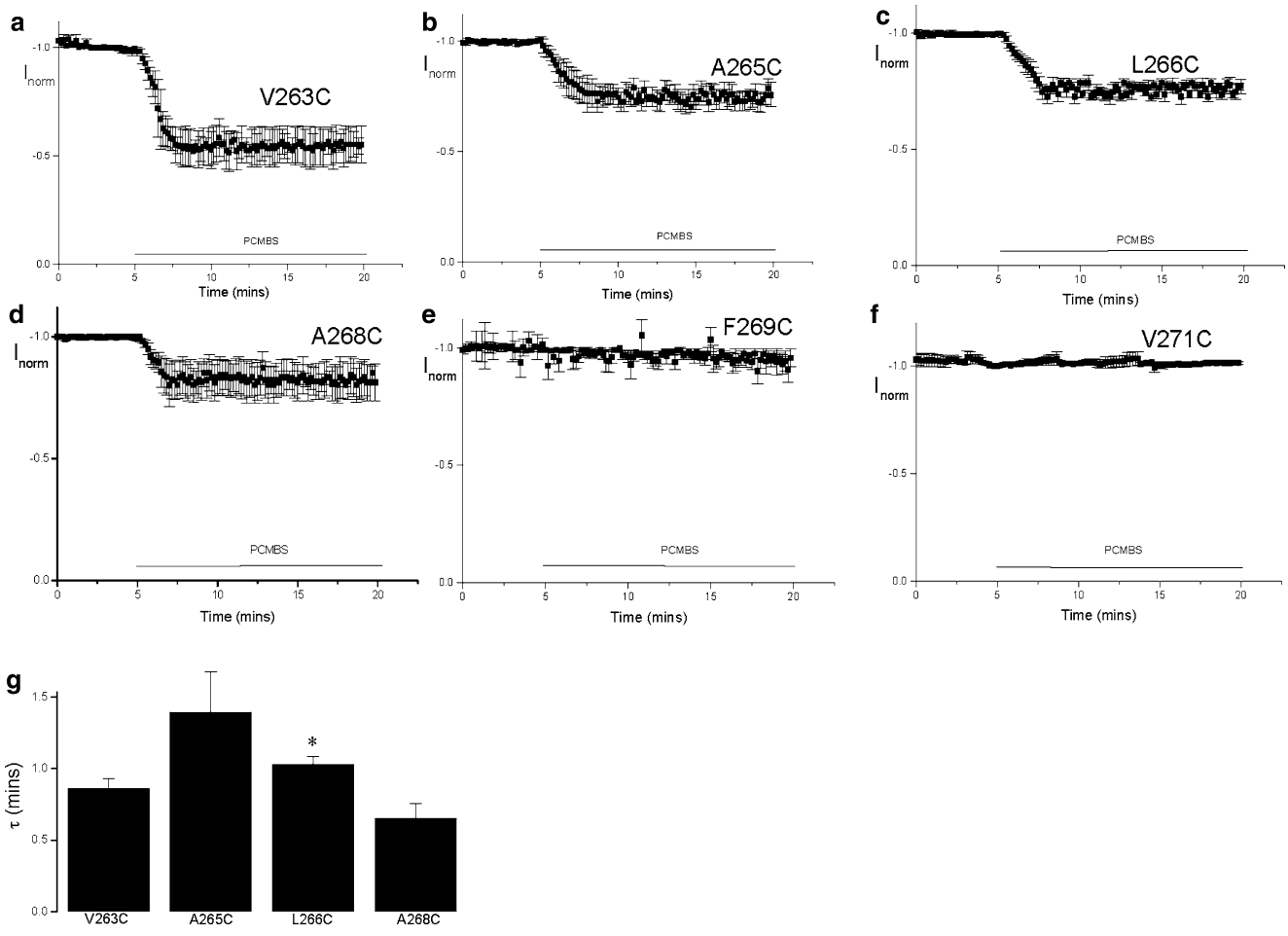

Fig. 8 Effects of PCMBS on calcium channels, with cysteine mutations in domain I S4 segment of chimera CGGG. **a**–**f** The effect of application of PCMBS (100 μM, indicated by the *bars*) on normalised currents for cysteine mutants V263C (*, −0.97 ± 0.05 μA, $n = 3$), A265C (*, −0.83 ± 0.01 μA, $n = 4$), L266C (*−0.86 ± 0.06 μA, $n = 3$), A268C (*, −0.95 ± 0.03 μA, $n = 3$), F269C (−0.81 ± 0.06 μA, $n = 4$), and V271C (−0.78 ± 0.08 μA, $n = 3$) during repetitive depolarisations (see "Materials and methods") from a holding potential of −80 mV. Paired Student's *t* tests were carried out (using initial and final values averaged over 5 min for each cell); significant reductions ($p < 0.05$) in current by PCMBS are denoted by asterisks in the data given above. **g** Exponential time constants, τ, of the time course of inhibition of PCMBS for V263C, A265C, L266C and A268C. An *asterisk* indicates significant difference ($p < 0.05$, analysis of variance test) for L266C as compared with A268C

movement of the pore region itself. Indeed, Talavera and coworkers (2001, 2003) made point mutations in the selectivity filter for $Ca_V3.1$, i.e. within the region covered by our chimera I-(P-S6)C, Fig. 6a, and showed that these mutations changed the voltage dependences of activation properties, consistent with our conclusion that pore domains are involved. However, our results indicate that it is not just the selectivity filter that is involved; for instance the S5-P region is not only involved in determining $V_{0.5}$ but is also involved in determining the slope parameter, k. Furthermore, although there is considerable homology in S5, P helix, selectivity filter and S6 (Fig. 6a), there is a long connecting loop between S5 and the P region for $Ca_V3.1$ (absent for $Ca_V1.2$) that may also contribute to differences. Moreover, since the activation gate of calcium channels is likely localised in the pore (e.g. Jurkat-Rott and Lehmann-Horn 2004), the gate may well reside in the S6 part of the P-S6 region that we have implicated, and so the gate itself may also directly affect the voltage dependence of activation.

In this study, we found that the functional characteristics of molecular regions of domain II are different from those of domain I. With the somewhat smaller influence of domain II on determining the voltage dependence of activation, both the voltage sensor S1–S4 region and the pore S5–S6 region of domain II contributed to determining the voltage dependence of activation. Indeed in our earlier work, we had shown that S4 of domain II makes a clear contribution (Li et al. 2004). One explanation for the different pattern of results for domain II as compared with domain I may be that, although domain II does not critically control calcium channel opening, it may modulate activation by coupling with domains I, III and IV via both S1–S4 and S5–S6 regions in domain II. For sodium channels, studies

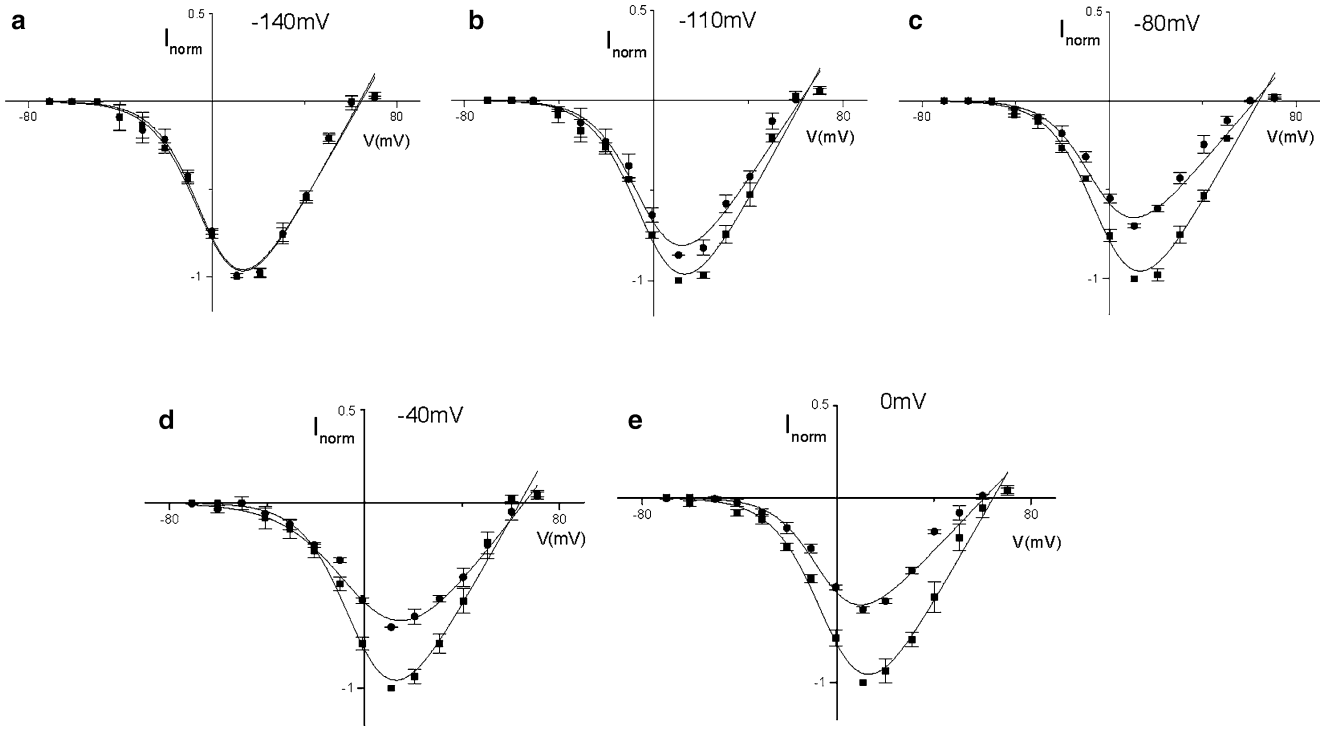

Fig. 9 Dependence on holding potential for inhibition of CGGG V263C by PCMBS. **a**–**e** Current/voltage curves for mutant V263C before (*squares*) and after (*circles*) application of PCMBS (100 μM). The reagent was applied in the absence of stimulation at the indicated holding potentials (see "Materials and methods"). Currents were normalised to the value at +10 mV before PCMBS application (−140 mV, −1.04 ± 0.09 μA, $n = 4$; −110 mV, −0.79 ± 0.08 μA, $n = 3$; −80 mV, −0.74 ± 0.02 μA, $n = 5$; −40 mV, −0.83 ± 0.05 μA, $n = 3$; 0 mV, −1.10 ± 0.08 μA, $n = 3$) and curves were fitted by Boltzmann curves. The Boltzmann parameters ($V_{0.5}$ and k) were not significantly affected by PCMBS treatment

using fluorescent tags showed that domains I, II and III are the key regions for channel activation, and movement of domain IV during activation is triggered by the other three domains (Chanda and coworkers 2002, 2004). It may be that a similar situation occurs for calcium channels, with movement of domain II being triggered by movement of the other three domains.

We also showed that the intracellular I/II linker does not contribute to determining whether the channel is high-voltage activating or low-voltage activating. In fact replacement of this linker in $Ca_V3.1$ by $Ca_V1.2$ in chimera I–II(L)C even shifted the I/V curves in a hyperpolarising direction rather than the opposite. The mechanism for this is unknown, but it may come about from an interfering effect of the linker on the IS6 region of the pore in the chimera. The $V_{0.5}$ value for activation of this chimera with $Ca_V3.1$ replaced by $Ca_V1.2$ at the I/II linker was not affected by auxiliary subunits, although such an action might have been expected from the known shift seen for $Ca_V1.2$ (Walker and De Waard 1998). It may be that other regions besides the I and II linker are also involved in β subunit action (such as the IS6 region), and indeed in a recent abstract (Arias et al. 2004), the nature of the linkage between the I/II linker and IS6 was also implicated in β subunit action.

Domains III and IV are also key regions in determining the voltage dependence of activation, as for domain I. Lin et al. (2004) showed that isoforms of the N-type channel $Ca_V2.2$ that are alternatively spliced in the S3–S4 region in domain IV do not show differences in the voltage dependence of activation, similar to the results we have found here for domain I. Thus, as for domain I, domain IV (and perhaps also domain III) may depend only on S5–S6 rather than S1–S4. It will be interesting to test this in further studies.

The inactivation gate has not yet been unambiguously localised in calcium channels. For domain I, our results show that the pore regions (S5-P and P-S6), rather than the S1–S4 region, determine inactivation properties. This is consistent with, and extends, our earlier results swapping domain I or IS4 (Li et al. 2004), and also with previous reports showing that S6 in domain I is important in determining the inactivation of calcium channels (Zhang et al. 1994; Bernatchez et al. 2001).

For domain II chimeras S1–S4 and S5–S6 with $Ca_V3.1$ replaced by $Ca_V1.2$, as well as for the I/II linker chimeras, inactivation remained transient, suggesting a less important role for domain II than domain I in the inactivation process. However, inactivation for these three chimeras was slower by around a factor of 2 than for wild-type $Ca_V3.1$, suggesting some kind of modulating role. Furthermore, swapping the whole of domain II and the I/II linker in $Ca_V3.1$ with $Ca_V1.2$ still produced an inactivating channel (Li et al. 2004), but with much slower inactivation than for the chimeras in domain II (swapping S1–S4 or swapping S5–S6) or for the

I/II linker chimera, suggesting that there may be interaction among these three regions (i.e. S1–S4, S5–S6 and the I/II linker) in determining inactivation. Indeed it has been reported that the I–II linker and the S6 region in domain II are involved in inactivation of calcium channels (Berrou et al. 2001; Geib et al. 2002; Park et al. 2004; Stotz and Zamponi 2001).

Of course, as is the case with any standard mutagenesis approach, it is conceivable that unforeseen spurious structural changes might occur in the chimeras we have constructed (such as alterations of interactions between subunits), which may provide an alternative, although unlikely, explanation of our results. Indeed, in our chimeras, we swapped homologous regions, except for the loop regions. Also the chimeras generally did not have anomalous properties; thus, the k values for the chimeras were not grossly different (apart from the I/II linker chimeras) from those for wild-type channels, as observed here or by others (Lacinova et al. 1999). Furthermore, the S4 movement of the domain I chimera was investigated and shown to be as expected, as discussed further in the following.

Study of the movement of the S4 segment of domain I chimera CGGG was carried out using cysteine-scanning mutagenesis, investigating accessibility to the cysteine-binding reagent PCMBS. Inhibitory effects of PCMBS were reversed by dithiothreitol, although not by washing, indicating specific effects of the reagent on cysteines. We showed that, under depolarising conditions, the S4 segment is exposed to the extracellular environment up to and including residue A268, with residues 269 and 271 remaining buried within the membrane. We also examined residue V263, and showed that this residue is accessible at depolarised, but not hyperpolarised, potentials. Thus, taken together, it appears that depolarisation causes the S4 region in domain I in this chimeric calcium channel to move outwards such that buried residues are exposed to the extracellular solution.

Our detailed study of residue 263 showed that there is movement of the S4 region even at a hyperpolarised potential (−110 mV) relative to the resting potential; an interpretation of this would be that at least one S4 segment of the channel must have been moved outwards by this hyperpolarised potential. However, although the protocol we used (i.e. with exposure to PCMBS for a fixed time) shows voltage-dependent movement of this residue in S4, time course experiments would be needed to quantitatively determine the $V_{0.5}$ value for this effect (and the same qualification applies to our earlier estimates of $V_{0.5}$ for Shaker using the same protocol, Yusaf et al. 1996). Even without quantitative analysis, the data indicate that movement of S4 in this calcium channel occurs at potentials more hyperpolarised than for ionic currents via the pore. Consistent with this, as previously mentioned, gating currents precede activation of both $Ca_V1.2$ and $Ca_V3.1$ channels.

Our data for residues 263, 265, 266, 268, 269 and 271 were obtained with repetitive depolarising pulses from a holding potential of −80 mV. Since the results show exposure of residue 263 even at hyperpolarised potentials, one may expect movement and hence accessibility to PCMBS even at the holding potential itself (as well as, more markedly, during the depolarising steps). However, as residue 263 showed voltage-dependent movement and residues 269 and 271 were not accessible under these depolarising conditions, it seems reasonable to assume that there is outward movement of the S4 helix as far as and including residue 268, but not beyond.

Our results add evidence to the correctness of the alignment of the S4 segment of Shaker with S4 of the $Ca_V1.2$ domain I from the CGGG chimera, as shown in Fig. 6c. Thus, residues up to and including A268 are exposed to the extracellular environment upon depolarisation in the CGGG chimera, which corresponds to exposure up to residue L366 of Shaker. Taking the membrane boundary at G260 (corresponding to Shaker L358, Gandhi and Isacoff 2002), this would correspond to a movement outwards of nine residues in the calcium channel. However, as it is thought that S4 lies in a water-filled crevice (Gandhi and Isacoff 2002), movement must be less than this, perhaps just up to V263, involving at least six residues. The S4 segment is well conserved between Shaker and this calcium channel; and by analogy with Shaker (Gandhi and Isacoff 2002), residues K264, R267, R270 and R273 of this calcium channel are likely to mainly contribute to gating charge measurements when S4 moves in this calcium channel. Overall, it can be seen that the movement of the S4 region in this chimeric calcium channel is as might be expected when compared with potassium channels. Furthermore, results that we have found for domain I S4 movement in this high-voltage activating chimera likely apply also to wild-type $Ca_V1.2$; clearly it would also be of interest to test S4 movement of $Ca_V1.2$ directly, and indeed to test S4 movement in domains II, III and IV.

In summary, we have studied domains I and II of calcium channels. Domain I is of key importance in determining whether the channel is low-voltage activating or high-voltage activating and in determining inactivation, and the molecular region that is important in determining these properties comprises both the S5-P and the P-S6 pore regions, but not the voltage sensor S1–S4 region. Domain II is of less importance in determining both the voltage dependence of activation and the inactivation properties than domain I, and by contrast with domain I, both the S1–S4 and S5–S6 regions are responsible for determining activation properties in domain II. We have shown that, upon depolarisation, the S4 segment of domain I of $Ca_V1.2$ moves such that amino acids up to residue 268 of S4 become exposed to the extracellular solution. This outward movement occurs at more hyperpolarised potentials than for ionic currents, corresponding to a movement of S4 segments before channel opening.

Acknowledgement We thank the Biotechnology and Biological Sciences Research Council for support.

References

Arias JM, Murbartian J, Perez-Reyes E (2004) Studies using chimeric LVA-HVA channels indicate that auxiliary β subunits modulate HVA channels through a direct coupling of the I–II loop and IS6 segments. Biophys J 86:273a

Bernatchez G, Berrou L, Benakezouh Z, Ducay J, Parent L (2001) Role of repeat I in the fast inactivation kinetics of the $Ca_V2.3$ channel. Biochim Biophys Acta 1514:217–229

Berrou L, Bernatchez G, Parent L (2001) Molecular determinations of inactivation within the I-II linker of α_{1E} ($Ca_V2.3$) calcium channels. Biophys J 80:215–228

Bezanilla F (2002) Voltage sensor movements. J Gen Physiol 120:465–473

Catterall WA (1995) Structure and function of voltage-gated ion channels. Ann Rev Biochem 64:493–531

Cha A, Ruben PC, George AL Jr, Fujimoto E, Bezanilla F (1999a) Voltage sensors in domains III and IV, but not I and II, are immobilized by Na^+ channel fast activation. Neuron 22:73–87

Cha A, Snyder GE, Selvin PR, Bezanilla F (1999b) Atomic scale movement of the voltage-sensing region in a potassium channel measured via spectroscopy. Nature 402:809–813

Chanda B, Bezanilla F (2002) Tracking voltage-dependent conformational changes in skeletal muscle sodium channel during activation. J Gen Physiol 120:629–645

Chanda B, Asamoah OK, Bezanilla F (2004) Coupling interactions between voltage sensors of the sodium channel as revealed by site-specific measurements. J Gen Physiol 123:217–230

De Waard M, Campbell KP (1995) Subunit regulation of the neuronal α_{1A} Ca^{2+} channel expressed in Xenopus oocytes. J Physiol 485:619–634

Ellis SB, Williams ME, Ways NR, Brenner R, Sharp AH, Leung AT, Campbell KP, McKenna E, Koch WJ, Hui A, Schwartz A, Harpold MM (1988) Sequence and expression of mRNAs encoding the alpha 1 and alpha 2 subunits of a DHP-sensitive calcium channel. Science 241:1661–1664

Gandhi CS, Isacoff EY (2002) Molecular models of voltage sensing. J Gen Physiol 120:455–463

Garcia J, Nakai J, Imoto K, Beam KG (1997) Role of S4 segments and the leucine heptad motif in the activation of an L-type calcium channel. Biophys J 72:2515–2523

Geib S, Sandoz G, Cornet V, Mabrouk K, Fund-Saunier O, Bichet D, Villaz M, Hoshi T, Sabatier JM, deWaard M (2002) The interaction between the I–II loop and the III–IV loop of $Ca_V2.1$ contributes to voltage-dependent inactivation in a beta-dependent manner. J Biol Chem 277:10003–10013

Glauner KS, Mannuzzu LM, Gandhi CS, Isacoff EY (1999) Spectroscopic mapping of voltage sensor movement in the Shaker potassium channel. Nature 402:813–817

Hofmann F, Lacinova L, Klugbauer N (1999) Voltage-dependent calcium channels: from structure to function. Rev Physiol Biochem Pharmacol 139:33–87

Horton RM, Hunt HD, Ho SN, Pullen JK, Pease LR (1989) Engineering hybrid genes without the use of restriction enzymes: gene splicing by overlap extension. Gene 77:61–68

Jiang Y, Lee A, Chen J, Ruta V, Cadene M, Chait BT, MacKinnon R (2003) X-ray structure of a voltage-dependent K^+ channel. Nature 423:33–41

Josephson IR (1997) Kinetic components of the gating currents of human cardiac L-type Ca^{2+} channels. Pflugers Arch 433:321–329

Jurkat-Rott K, Lehmann-Horn F (2004) The impact of splice isoforms on voltage-gated calcium channel alpha1 subunits. J Physiol 554:609–619

Klugbauer N, Marais E, Lacinova L, Hofmann F (1999) A T-type calcium channel from mouse brain. Pflugers Arch 437:710–715

Lacerda AE, Perez-Reyes E, Wei X, Castellano A, Brown AM (1994) T-type and N-type calcium channels of Xenopus oocytes: evidence for specific interactions with β subunits. Biophys J 66:1833–1843

Lacinova L, Klugbauer N, Hofmann F (1999) Absence of modulation of the expressed calcium channel α_{1G} subunits by α_2-δ subunits. J Physiol 516:639–645

Lacinova L, Klugbauer N, Hofmann F (2002) Gating of the expressed $Ca_V3.1$ calcium channel. FEBS Lett 531:235–240

Larsson HP, Baker OS, Dhillon DS, Isacoff EY (1996) Transmembrane movement of the Shaker K^+ channel S4. Neuron 16:387–397

Li J, Stevens L, Klugbauer N, Wray D (2004) Roles of molecular regions in determining differences between voltage dependence of activation of $Ca_V3.1$ and $Ca_V1.2$ calcium channels. J Biol Chem 279:26858–26867

Lin Y, McDonough SI, Lipscombe D (2004) Alternative splicing in the voltage-sensing region of N-type $Ca_V2.$ 2 channels modulates channel kinetics. J Neurophysiol 92:2820–2830

Mikami A, Imoto K, Tanabe T, Niidome T, Mori Y, Takeshima H, Narumiya S, Numa S (1989) Primary structure and functional expression of the cardiac dihydropyridine-sensitive calcium channel. Nature 340:230–233

Neely A, Wei X, Olcese R, Birnbaumer L, Stefani E (1993) Potentiation by the β subunit of the ratio of the ionic current to the charge movement in the cardiac calcium channel. Science 262:575–578

Park JY, Kang HW, Jeong SW, Lee JH (2004) Multiple structural elements contribute to the slow kinetics of the $Ca_V3.3$ T-type channel. J Biol Chem 279:21707–21713

Perez-Reyes E, Castellano A, Kim HS, Bertrand P, Baggstrom E, Lacerda AE, Wei XY, Birnbaumer L (1992) Cloning and expression of a cardiac/brain beta subunit of the L-type calcium channel. J Biol Chem 267:1792–1797

Perez-Reyes E (2003) Molecular physiology of low-voltage-activated T-type calcium channels. Physiol Rev 83:117–161

Scholze A, Plant TD, Dolphin AC, Nurnberg B (2001) Functional expression and characterization of a voltage-gated $Ca_V1.3$ (α_1D) calcium channel subunit from an insulin-secreting cell line. Mol Endocrinol 15:1211–1221

Sheets MF, Hanck DA (2002) The outermost lysine in the S4 of domain III contributes little to the gating charge in sodium channels. Biophys J 82:3048–3055

Singer D, Biel M, Lotan I, Flockerzi V, Hofmann F, Dascal N (1991) The roles of the subunits in the function of the calcium channel. Science 253:1553–1557

Stotz SC, Zamponi GW (2001) Identification of inactivation determinants in the domain IIS6 region of high voltage activated calcium channels. J Biol Chem 276:33001–33010

Talavera K, Staes M, Janssens A, Klugbauer N, Droogmans G, Hofmann F, Nilius B (2001) Aspartate residues of the Glu-Glu-Asp-Asp (EEDD) pore locus control selectivity and permeation of the T-type Ca^{2+} channel alpha(1G). J Biol Chem 276:45628–45635

Talavera K, Janssens A, Klugbauer N, Droogmans G, Nilius B (2003) Pore structure influences gating properties of the T-type Ca^{2+} channel alpha 1G. J Gen Physiol 121:529–540

Walker D, De Waard M (1998) Subunit interaction sites in voltage-dependent Ca^{2+} channels: role in channel function. Trends Neurosci 21:148–154

Wray D (2000) How to communicate with a cell. Sci Spectra 23:64–71

Yamaguchi H, Muth JN, Varadi M, Schwartz A, Varadi G (1999) Critical role of conserved proline residues in the transmembrane segment 4 voltage sensor function and in the gating of L-type calcium channels. Proc Natl Acad Sci USA 96:1357–1362

Yusaf SP, Wray D, Sivaprasadarao A (1996) Measurement of the movement of the S4 segment during the activation of a voltage-gated potassium channel. Pflugers Arch 433:91–97

Zhang JF, Ellinor PT, Aldrich RW, Tsien RW (1994) Molecular determinants of voltage-dependent inactivation in calcium channels. Nature 374:97–100